Larvae of grassland caterpillar endemic to Qinghai–Tibet Plateau (Lepidoptera: Lymantriinae: Gynaephora): identification, distribution, and ultramorphology

Chen Yuan
Qinghai University
Hainan Shao
Qinghai University
Jinping Fu
Qinghai University
Siyu Liu
Qinghai University
Yunxiang Liu
17791394452@163.com

Qinghai University

Article

Keywords:

Posted Date: February 22nd, 2024

DOI: https://doi.org/10.21203/rs.3.rs-3893693/v1

Additional Declarations: No competing interests reported.

Abstract

The grassland caterpillar is a significant pest of alpine meadows in the Qinghai-Tibet Plateau. Its larvae primarily feed on forage grasses, resulting in financial losses. However, little research has been done on the morphological features of larvae of this species thus far. The distribution and habitat of *Gynaephora menyuanensis* were extensively investigated in this instance through field study. Using an optical and scanning electron microscope(SEM), the external morphology and ultramorphology of the last instar larvaeof *G. menyuanensis*were investigated. The findings indicate that this species is primarily found in the northeast of Qinghai Province in alpine meadows at an altitude of 3,000–3,500 m. For the first time, SEM is used to report more comprehensive morphological structuresof *G. menyuanensis*, including larval head capsule, mouthparts, antenna, sensilla, thoracic legs, prolegs, and setae. The larvae have two distinct color funnel warts (yellow and red) on abdominal segments VI and VII, which sets them apart from other lepidopterous larvae. Additionally, the chaetotaxy of first instar larvae of *G. menyuanensis* were studied and described in detail, identifying seven clusters(PD, D, SD, L, SV, V, CV) on the larval trunk. This study offers a theoretical basis for phylogenetic analysis, the adaption evolution of *G. menyuanensis*, and a systematic discussion of the application of morphological features of larvae to classification.

Introduction

The Lymantriinae family has approximately 2,500 species arranged in 360 genera, commonly called tussock moths. During its larval stage, most Lymantriinae species are arboreal defoliators and frequently polyphagous1,2. Some are significant pests in agriculture and animal husbandry, such as *Arna pseudoconsperas* Strand, *Orgyis antiqua* Linnaeus (vaporer or rusty tussock moth)3,4. *Gynaephora* is a tiny genus belonging to the Lymantriinae subfamily, primarily found in the high mountainous areas of the Northern Hemisphere and the Arctic tundra5,6. There are now 15 species of *Gynaephora* worldwide, including eight in China7,8. Despite their allopatric distribution, the phylogenetics and species delimitation in the genus Gynaephora have generated controversy[5,7].

The endemic *G. menyuanensis* of the Qinghai–Tibet Plateau (QTP) has gained a reputation as a devastating pest that harms the ecosystem of alpine meadows and the advancement of animal husbandry[8]. More than 20 forage grasses, including *Elymus nutans* Griseb, *Stipa capillata* L., *Artemisia lancea* Vaniot, *Poa crymophila* Keng, and *Ceratoides latens* Tourn, are consumed by its voracious larvae in QTP, where infestations cause 20%–80% loss of alpine meadows loss and contribute to their degeneration9. Remarkably, *G. menyuanensis* has evolved apparent morphological features in QTP to adapt to low temperatures (low supercooling points) and high ultraviolet (UV) radiation (black bodies)10. To survive in the harsh environment, grassland caterpillars overwinter as first instar larvae under grassroots or cow dung. Several studies have revealed that many species have acquired morphological features to adapt to their particular environments6. Most recent research has been on mitochondrial

genes associated with the adaptive evolution of *G. menyuanensis*[5]. Nevertheless, very little is known about the identification, distribution, and detailed morphological features of *G. menyuanensis*.

The life history of holometabola insects, which significantly influence the production and development of agriculture and forestry, especially during the larval period[11]. Larvae avoid competition with other species by occupying distinct ecological niches12. The morphology and feeding habits of larvae, the larvae of holometabolous insects, are very different from those of adults13. Due to the high diversity of morphological characteristics among groups, particularly in Lepidoptera, larval morphology might yield useful features for insect taxonomic and phylogenetic analyses[14]. In recent years, the morphological features of larvae have become more critical in the phylogenetic analysis of different holometabolic insect groups[15]. The examination of the evolutionary history of this group is facilitated by several characteristics proposed by Cardoso, including the presence of crochets in Smerinthinae and Sphingidae, as well as the order of larval hair tufts[16]. Nonetheless, the larval morphology is relatively inadequate compared to their adult forms.

To help safeguard the fragile ecosystems, our study used external morphology and molecular technology to identify the larvae samples and determine their distribution over the Tibetan Plateau. Furthermore, we used light and scanning electron microscopy to describe the morphology and chaetotaxy of *G. menyuanensis* larvae for the first time, adding to the body of evidence for larval identification and illuminating the underlying defensive mechanisms of these grassland caterpillars.

Results

Identification

The morphological features described by Yan are entirely comparable with the white and orange-red markings on the abdominal intersegmental membrane of the last instar larvae of *Gynaephora menyuanensis*, which also have black abdominal prolegs and an anterior pectoral backplane[8] (Fig. S1). Furthermore, there was a significant decrease in the intraspecific genetic distances of 0–0.0012 (n = 20) and the nucleotide similarity with the reference sequences of 99.8% compared to the inter-species genetic distances of 0.03 of Lepidoptera[17]. The individuals acquired in our study are all members of the same species, i.e., *G. menyuanensis* Yan et Chou (Lepidoptera: Lymantriinae), based on molecular and morphological identifications.

Distribution and habitats

The primary distribution regions of *G. menyuanensis* are parts of Gansu (Minle, Sunan, and Jishishan) and the northeastern alpine meadow areas of Qinghai (Menyuan, Qilian, Haiyan, Tianjun, Datong, Huzhu, Ledu, Hualong, Xunhua, Tongren, Guide, Gonghe, Xinghai, Tongde, and Guinan) (Fig. 1A, B). The habitats have an average height of more than 3,000 m, an average annual temperature of 0.6°C, and an annual

precipitation of ~ 530 mm (Fig. 1). In particular, ~ 55% of the annual precipitation falls in June, July, and August, corresponding to a typical continental plateau climate. The plant growth period spans approximately 135 days annually. According to our findings, *G. menyuanensis* was more abundant near streams (Fig. 1C), and (Fig. 1D) they primarily consumed high-quantity forage, including Gramineae and Cyperaceae (Fig. 1D).

Morphology of the last instar larvae

The general body morphology

Gynaephora menyuanensis larvae in their last instar are usually eruciform, with a head, thorax, and abdomen (Fig. S1A). With three pairs of thoracic legs, four pairs of abdominal prolegs, and one pair of anal prolegs, its cylindrical trunk contains 13 segments (Fig. S1B, C). There are prominent hair tufts with dense black setae covering the dorsal surface. With a pair of metathoracic spiracles and eight pairs of abdominal spiracles on A1–A8, the respiratory system is of the peripneustic type. There is a pair of funnel warts on abdominal segments VI to VII, a hallmark of the Lymantriinae family. The abdominal intersegmental membrane of *G. menyuanensis* has white and red speckles that can be used to identify it from other species of *Gynaephora* (Fig. S1B).

The head

With an inverted Y-shaped ecdysial line on the midcranium measuring 3.519 ± 0.52 mm (n = 60) in width (Fig. 2A, B, D), the hemispherical and sclerotized head turns positive red with the increase of larva instar (Fig. 2). There are a lot of bristles on the dorsal surface of the head (Fig. 2). Six pairs of protuberant stemmata were symmetrically arranged behind the antennae (Fig. 2B, C). The antennae, which are located laterally behind the mandibles, are divided into three segments: a well-developed basal scape located in the antennal fossa, a longest pedicel, and a cone-shaped and the shortest flagellum at the end of the pedicel (Fig. 3A).

The mandibulate variety of mouthparts includes a labrum, a pair of mandibles, a pair of maxillae, and a labium (Fig. 3B). The clypeus, which has six pairs of setae on its external surface, is connected to the labrum, which is a flat, medially notched structure (Fig. 3C). To assist the larvae in feeding the grass. The labrum can move back and forth. The paired mandibles have complementary heavy sclerotization and asymmetrical shapes (Fig. 3C). The cutting end has a pair of setae on the external surface and is wavy with four sharp ends for shredding food (Fig. 3D). On the labium, the paired maxillae are symmetrically positioned. Each maxilla's primary purpose, comprising a cardo, stipes, galea, and a maxillary palp, is to grab food and facilitate chewing. The center between the paired maxillae is covered in many triangular-shaped spicules with sharp ends (Fig. 3E). A pair of labial palps and a spinneret are provided by the labium (Fig. 3F). Silk is secreted from a hole at the top of the spinneret, a cuticle-covered tubular structure that protrudes from the anterior of the labium.

Types of sensilla in the antenna and mouthparts

The mouthparts under SEM reveal the morphological traits of four distinct types of sensilla (Figs. 4, S2; Table 1):

Table 1
Morphological features of the sensilla on the antenna and mouthparts of the last instar larva of *G. menyuanensis*.

Type of sensillum	Length/μm	Base width/ μm	Tip	Wall
Sensilla trichodea I (Str I)	106.72 ± 9.97	11.11 ± 1.36	Trichoid	Smooth
Sensilla trichodea II (Str II)	205.55 ± 19.42	25.81 ± 1.97	Trichoid	Smooth
Sensilla chaetica I (Sch I)	39.97 ± 3.25	13.01 ± 3.87	Sharp	Smooth
Sensilla chaetica II (Sch II)	16.33 ± 2.23	6.41 ± 1.21	Sharp	Smooth
Sensilla basiconica I (Sb I)	5.63 ± 2.08	4.51 ± 0.38	Blunt	Oblique striation, Porous
Sensilla basiconica II (Sb II)	31.07 ± 2.83	15.22 ± 0.42	Blunt	Smooth
Sensilla styloconica I (Ss I)	24.60 ± 1.34	12.86 ± 0.85	Blunt	Smooth
Sensilla styloconica II (Ss II)	19.98 ± 2.65	13.40 ± 1.76	Blunt	Smooth, Porous

Sensilla trichodea (Str, two subtypes: Str I, Str II); Sensilla chaetica (Sch, two subtypes: Sch I, Sch II); Sensilla styloconica (Ss, two subtypes: Ss I, Ss II); and Sensilla basiconica (Sb, two subtypes: Sb I, Sb II).

Located on the mouthparts of *G. menyuanensis* larvae in their last instar, Str are the most prevalent sensilla. With an end that resembles hair, the Str I are located near the apex of the antennal pedicle. Str II are more prolonged than Str I and located on the surface of the maxillae and apex of the antennal pedicle (Fig. 4A; Table 1). At the midpoint, the Str II are helical.

Sch have two kinds, primarily located on the ventral side of the larval antennae: long Sch (Sch I) and short Sch (Sch II). Sch I are found near the base of the antennal flagellum and maxillary galea, and they progressively taper to the blunt tip with smooth cuticles. The Sch II are nearly perpendicular to the antennal surface and are gathered on the antennal pedicle's surface (Fig. 4B). Sch I and Sch II have mean lengths of 39.97 ± 3.25 μm and 16.33 ± 2.23 μm, respectively, and the basal widths of 13.01 ± 3.87 μm and 6.41 ± 1.21 μm, respectively (Table 1).

Ss can be divided into two types based on their shapes. Ss I have a smooth surface without any visible wall pores at the top of the antennal flagellum and a thin and pointed cone protrusion at the blunt distal points. Ss II have a smooth surface on the maxillary galea and a blunt tip papillary protrusion (Fig. 4C).

The basal widths of Ss are 12.86 ± 0.85 μm and 13.40 ± 1.76 μm, respectively, and the mean lengths are 24.60 ± 1.34 μm and 19.98 ± 2.65 μm (Table 1).

The apex of the Sb is rounded and blunt. Sb I are found on the antennal flagellum's surface and the maxillary palp's apex. The columnar Sb I have oblique striations and several tiny, uneven, wrinkle-shaped pores at their blunt tips and hidden sockets. Longer and more robust than Sb I, Sb II is primarily located in the maxillary basal fossa and antennal pedicel. The Sb II has sharp tips and smooth walls without detectable depressions (Fig. 4D; Table 1).

Thoracic legs and prolegs

Three thoracic legs (Fig. 5A, B), each of the thoracic leg is composed with a coxa, femur, tibia, tarsus, and pretarsus (Fig. 5C). The thickest coxa is covered with dense hair. The femur and longest tibia have several setae on their lateral surfaces, whereas their anterior surfaces are usually glabrous. The tarsus is subconical in shape and has two short setae, five short sensilla chaetica, and a terminally curved, pointed pretarsus (Fig. 5D).

The unsegmented abdominal prolegs consist of proximal and distal bases and are located on abdominal segments III and VI (Figs. 5E, S3). Several setae cover the lateral and mesal surfaces of the proximal base (Figs. 5E, 6A, S3). Mesally, the planta are covered in dense microtrichia (Fig. 6D). The apical planta of prolegs have 17–25 uniform crochets arranged in a mesal penellipse (Figs. 6A–D, S4). Except for the number of crochets, the anal and abdominal prolegs have similar structures.

Setae on the trunk

The grass caterpillar larvae are covered by dense hair tufts, on where several setae insert (Fig. 7A, E). On the last instar larvae, there are three main types of setae: needle-shaped, spiral-shaped, and penniform (Fig. 7B, C, D). Compared to spiral-shaped setae, penniform setae are longer and have dense microtrichia. When touched, the hollow setae can break readily and irritate the skin (Fig. 7F). In addition to helping the larvae crawl and spread, the setae can be used to identify the taxonomic status of the larvae based on the number and arrangement of their hair tufts.

Funnel warts

On abdominal segments VI to VII, the larval funnel warts display two distinct colors: red (: n = 29a, : n = 27a) and creamy yellow (: n = 20a, : n = 21a) (Fig. 8A–D). The findings showed no correlation between the gender of *G. menyuanensis* and the intraspecific color differences of funnel warts (χ^2 = 0.003, *P* = 0.956). The funnel warts have an oval, volcano-shaped aperture. At the proximal opening of the funnel, furrows and a few secretions are visible (Fig. 8C, D). When viewed from within the larva, prominent muscle insertion points may be seen at the bottom of the funnel, and many trichomes are visible only inside. The larvae's body will curl into a ball, and their versible osmeterium will expand outward to form a papillary bulge in response to external stimulation. According to the ultrastructure, many well-developed

secretory cells are connected to the hollow column-shaped organ dispersed across the gland's surface (Fig. 8E, F).

Chaetotaxy of the first-instar larvae

For the left side of the body, the chaetotaxy of the first larval trunk is shown (Figs. 9, S5). Chaetotaxy on tathorax (T1–T3) and the abdominal segments 1–10 (A1–A10) show similar setal arrangement.

Prothorax (T1)

The prothorax bears an enormous prothoracic shield, on which are three setigerous tubercles: dorsal cluster (D), subdorsal cluster (SD), and lateral cluster (L). With 22 setae, the dorsal cluster (D) is anterior to the subdorsal cluster (SD). There are 20 setae on the lateral cluster (L) and 24 on the subventral cluster (Table 2; Figs. 9, S5). Each seta is a single, equal-length stiff filament that rises directly from the cluster.

Table 2
The number of setae in each segment and the setigerous tubercle of the first instar larva of *G. menyuanensis*.

Segments	PD	D	SD	L	SV	V	CV
T1	/	22	24	20	/	/	/
T2-T3	/	22	12	14	9	/	/
A1-A2	3	18	18	11	8	3	1
A3-A4	3	18	18	11	8	/	/
A5-A6	/	18	18	11	8	/	/
A7	/	18	16	11	8	3	1
A8	3	18	16	11	/	3	1
A9	/	18	16	8	/	3	1
A10	/	7	/	3	/	/	/

Meso- and meta- thorax (T2, T3)

In chaetotaxy, the meso- and meta-thorax are identical. The single bristle inserts on the dorsal cluster (D), subdorsal cluster (SD), lateral cluster (L), and subventral cluster (SV). With 22 setae, the setae rising from the dorsal cluster (D) are significantly more noticeable than the rest. The subdorsal cluster (SD) and lateral cluster (L) have 12 and 14 bristles, respectively. The subventral cluster (SV) has the smallest number of setae, with 9 bristles (Table 2; Figs. 9, S5).

Abdominal segments 1 and 2 (A1, A2)

Regarding chaetotaxy, the first two abdominal segments are the same in that they lack any appendages. Very noticeable setae rise from the dorsal cluster (D) and subdorsal cluster (SD). With 3 setae, the predorsal cluster (PD) is located anterolateral to the abdominal prolegs. With 11 setae, the lateral cluster (L) is anterior to the prothoracic spiracle. There are 3 shorter setae in the ventral cluster (V) and 8 in the subventral cluster (SV). On these segments, the central ventral seta (CV) is the shortest (Table 2; Figs. 9, S5).

Abdominal segments 3 and 6 (A3–A6)

Except for the absence of the V and CV clusters, the morphology of the A3 and A4 segments is identical, with five different types of clusters (PD, D, SD, L, and SV) that follow the same pattern as the A1 and A2 segments. A5 and A6 segments had the identical morphology as A3 and A4, with four types of clusters (D, SD, L, and SV), except for the absence of predorsal cluster (PD) (Table 2; Figs. 9, S5).

Abdominal segment 7 (A7)

Segment A7, with six types of clusters (D, SD, L, SV, V, and CV), is similar to that in segments A1 and A2, other than the absence of a predorsal cluster (PD) (Table 2; Figs. 9, S5).

Abdominal segment 8 (A8)

The setal arrangement and number of bristles originating from the predorsal cluster (PD), dorsal cluster (D), subdorsal cluster (SD), lateral cluster (L), ventral cluster (V), and central ventral cluster (CV) on A8 are the same as those on A1 and A2, except for the lack of a subventral cluster (SV) (Table 2; Figs. 9G, S5).

Abdominal segment 9 (A9)

The setae on A9 are comparably shorter, and the number of setae ascending from dorsal cluster (D), subdorsal cluster (SD), ventral cluster (V), and central ventral cluster (CV) are identical to that on A8 except for the lateral cluster (L: 8) (Table 2). The predorsal cluster (PD) and the spiracle are lacking compared to the setae layout on A8 (Figs. 9G, S5).

Abdominal segment 10 (A10)

The dorsal cluster (D) and the lateral cluster (L) are located on the dorsal sclerite of A10. Although the dorsal cluster (D) has a large surface area, it only has seven bristles. The lateral seta (L) is located ventral to the anal proleg with three setae (Figs. 9G, S5F).

Discussion

The most destructive pest of alpine meadows is *Gynaephora menyuanensis*, an indigenous species of the Qinghai-Tibet Plateau that feeds on high-quality forage. The high density of larval distribution, extensive occurrence area, and severe degree of injury result in the destruction of grassland vegetation, pose a risk to livestock stomatitis and significantly compromise livestock productivity while degrading

alpine meadows[6]. For the first time, SEM and morphological observations were used to examine the morphology of *G. menyuanensis* larvae in their last instar. The black setae trunk, positive redhead capsule, and a pair of red or creamy yellow funnel warts on the abdominal segment (Fig. S1) identify the larvae of the grass caterpillar from other larval genera. This unique morphology of the larvae is unique among the Lymantriidae.

Insect sensilla are essential for sensing sex pheromones and plant volatile in the environment, courtship, mating, and oviposition[18–20]. Through SEM observation, we were able to identify four types of sensilla (Figs. 3, 4, S2; i.e., Sensilla basiconica, Sensilla chaetica, Sensilla trichodea, and Sensilla styloconica) on the antennae and mouthparts of the mature larvae of *G. menyuanensis*. These types of sensilla are morphologically similar to other Lepidoptera larvae that have been previously reported (e.g., Noctuidae[21], Papilionidae[22], Carposinidae[23], and Sesiidae[24]). We identified two varieties of Sensilla trichodea in the antennae and maxillae. Their smooth walls and tips, devoid of depressions, suggest a mechanoreceptor function, and their positions suggest that these sensilla may be chemosensory receptors to taste food. According to research on the antennal sensilla of *Holcocerus hippophaecolus*, the primary functions of Sensilla chaetica is to sense physical and mechanical stimuli, choose which mechanical stimulation of the external environment to apply, and coordinate the movement of the mouthparts[25]. Additionally, we discovered that Sensilla basiconica (Sb I) are oblique striation-welled with many minute irregular wrinkle-shaped pores at their blunt tips. These pores serve an olfactory purpose that aids larvae in searching for and locating host plants[26]. Several studies have suggested that Sch are probably mechanoreceptors that coordinate the movement of the mouthparts and monitor the texture of the food[27]. Various morphological traits of Sensilla chaetia, Sensilla styloconic, and Sensilla basiconic have been observed on the antennae in this study (Fig. 4). Together with olfactory receptors, these sensilla may be involved in the movement of the maxillae and labium, and the detection of food or tunnel structure.

The prolegs are morphologically different among families, adapted to be highly strong and powerful in Saturniidae and Sphingidae[28] and deteriorated in Geometridae and some Noctuidae[13]. Three pairs of thoracic legs, each with a sharp pretarsus terminally, are present in the final instar larvae of *G. menyuanensis* (Figs. 5, S3). The strong thoracic legs of herbivorous insects can support the entire body during feeding, and they also function as the center of movement when the larvae are resting on the plant's surface[29]. Moreover, the unsegmented prolegs of the last instar larvae feature 17–25 crochets, while the first instar larvae only have four crochets (Figs. 6, S4). We assume that the morphological features of the thoracic and abdominal legs could have something to do with the local environment and host plants (Figs. 1, 5, S4). One primary characteristic that sets Lepidopteran larvae apart from other polypod larvae is their crochets[30]. Our findings indicate that the number of crochets on *G. menyuanensis* larvae increases progressively from the first to the last instar, which can be used to identify the larval instars.

In Lepidoptera, setae are primarily seen on the head and trunk of the caterpillar[31]. The setae usually specialized into stinging spines in Limacodidae[32] or assembled as dense tufts as mimicry of some

Arctiidae, Lasiocampidae, and Lymantriidae[33]. The larvae of *G. menyuanensis* are covered by large hair tufts, which carry many setae. The hypothesis is that the venomous, itchy setae act as insulation against the cold weather[4]. In QTP, the black setae may also shield *G. menyuanensis* from harmful UV radiation. In particular, in QTP, where habitats cannot provide shelter, grass caterpillars' setae, which are sensitive to touch, substrate, and air-borne vibrations, transmit mechanosensory information that includes intraspecific communication between individuals or early warning of the approach of enemies such as parasitoid wasps that wish to lay their eggs on or into their bodies.

Red or creamy yellow funnel warts are present on the last instar larvae of *G. menyuanensis* (Fig. 8). This is a valuable and unusual defense mechanism; when the larvae are stimulated externally, their bodies curl into a ball, and their versible osmeterium emerges as a papillary bulge. Through the use of SEM, Deml and Dettner examined the morphology of the funnel warts of four lymantriid species: *Lymantria dispar, L. monacha*, *L. concolor*, and L2 larvae of *Euproctis chrysorrhoea*[34,35]. An exceptionally high potential exists for classifying the connections among the Lymantriidae based on the morphology of the funnel warts[36]. The authors realized the funnel warts are essentially orifices of exocrine glands that secrete the substance. Chemical analyses of the secretions of the above-mentioned *Lymantria* spp. revealed that they contain several aromatic compounds (e.g., benzaldehyde and phenylacetaldehyde), N-containing compounds (e.g., pyrazines, 2-pyrrolidinone and nicotine), organic acids, and other chemicals such as glycerol and isopropyl myristate[37,38]. The secretions may work as a chemical defense against enemies, enhancing the protective properties of the hair tufts that cover many Lymantriid larvae[39]. Meanwhile, we discovered that gender had no bearing on the variation in color of *G. menyuanensis* funnel warts. Thus, more investigations are needed to determine the underlying molecular mechanism of the color change of the funnel warts and its application in the integrated pest management of this grass caterpillar.

Materials and methods

Insect collection and rearing

The grassland caterpillar occurrence sites in Qinghai and Gansu Provinces were examined every 6 days from March to August 2023 (Fig. 1). The larvae in their first and last instars were housed in the Qinghai University laboratory after being placed in plastic boxes (diameter 4 cm, height 12 cm), according to the sampling areas. All the samples were kept in an incubator at 18.0°C ± 2.8°C and a relative humidity 60% ± 10%. Seedlings of *Stipa capillata* L. and *Artemisia lancea* Vaniot were purchased from Suqian Verdara Green Engineering Co., Ltd., China, and cultivated in the green house of Qinghai University until the forage grasses grow to 20cm. The fresh grasses were fed to the grassland caterpillar larvae, and daily records of the molting time and pupation time were made[40].

Identification

The larvae samples were identified by external morphology and molecular technology. Using the Biospin insect genomic DNA extraction kit (Bioer Technology Co., Ltd., Hangzhou, Chian), 13 last instar larvae

from each sampling location were selected, and the DNA was extracted. Cytochrome c oxidase subunit I (*COI*: LCO1490-GGTCAACAAATCATAAAGATATTGG, HCO2198-TAAACTTCAGGGTGACCAAAAAATCA) was amplified[41]. A total of 25 μL was used in the polymerase chain reaction (PCR) system. The procedures were initial denaturation at 95°C for 2 minutes, then 95°C, 30 seconds, 30 cycles, followed by annealing at 52°C for 1 minute, extension at 72°C for 1 minute, and finally extension at 72°C for 10 minutes. To confirm that the PCR results were the intended target fragments, the products were identified using 1.0% agarose gel electrophoresis. For sequencing, Shanghai Sangon Biological Engineering Technology received the qualified DNA products. Sequence chromatograms were aligned in Clustal X v2.0.21 after being examined with Chromas Pro v2.23 (Technelysium Pty Ltd., Australia)[42]. BioEdit v7.0.9.0 was used to manually remove the gappy columns at the beginning and end of the alignment[43]. Using MEGA v6 to compute the genetic distance between interspecies, the nucleotide similarity with reference sequences—obtained by retrieving DNA barcode data from the Barcode of Life database (BOLD Systems v4, www.boldsystems.org)—was determined[44]. The grassland caterpillar *COI* sequences used in this study were entered into the GenBank database under the accession numbers PP238621–PP238625. The reference sequences were downloaded from the GenBank database (accession numbers KF887535–KF887540).

Morphological observation

Gynaephora menyuanensis larvae in their first and last instars were washed with 0.1 mol/L (pH = 7.4) phosphate buffer and dried at room temperature. A Nikon SMZ1500 stereomicroscope (Nikon Corporation, Tokyo, Japan) was used to examine the external morphology of the specimens and a Scientific Digital micrography system equipped with an Auto-montage imaging system and a QIMAGING Retiga 4000R digital camera (QImaging, Surrey, BC, Canada) was used to take photographs.

The larvae in their first and last instars were fixed in hot Dietrich's solution (formalin: 95% ethanol: glacial acetic acid: distilled water = 6:15:1:80, v/v) for the scanning electron microscope. They were then allowed to stand for 24 hours at room temperature under a fume hood before being preserved in 75% ethanol[45]. After being dehydrated for 20 minutes in a series of ethanol baths (30%, 50%, 70%, 80%, 90%, 95%, and 100%), larvae were freeze-dried for 4 hours, sputter coated with gold, and studied under a scanning electron microscope (JEOL 7900F) at 5 kV[46].

Declarations

Conflict of Interest

The authors have no conflicting interests.

Author declarations

The plant collection and use were in accordance with all the relevant guidelines.

Funding

The Natural Science Foundation of Qinghai Province (Grant No. 2022-ZJ-981Q) and the National Natural Science Foundation of China (Grant No. 32160263) funded this study.

Author Contribution

C.Y., H.N.S. and Y.X.L. conceptualized and designed the study. C.Y., J.P.F., S.Y.L. and Y.X.L. prepared all the figures and analyzed the data. C.Y., H.N.S. and Y.X.L. discussed the results and wrote the original draft. C.Y., H.N.S. and Y.X.L. critically revised the manuscript. All authors have read and agreed to the published version of the manuscript.

Acknowledgments

We appreciate Dr. Luchao Bai (Qinghai University, Xining, China) for kindly providing the optical microscope.

Data Availability Statement

Nucleotide sequences supporting the conclusions of this study can be found by the accession numbers (PP238621–PP238625), at NCBI GenBank: https://www.ncbi.nlm.nih.gov/nuccore/. Other data will be provided upon request to the corresponding author.

References

1. Wang, H. et al. Molecular phylogeny of Lymantriinae (Lepidoptera, Noctuoidea, Erebidae) inferred from eight gene regions. Cladistics 1–14 (2015).
2. Holloway, J. D. The moths of Borneo (part 5): family Lymantriidae. Malayan Nat. 53, 1–188 (1999).
3. Ziemnicka, J. Outbreaks and natural viral epizootics of the satin moth *Leucoma salicis* L. (Lepidoptera: Lymantriidae). Plant Prot. Res. 48, 23–38 (2008).
4. Uhlikova, H., Nakladal, O., Jakubcová, P. & Turčáni, M. Outbreaks of the Nun Moth (*Lymantria monacha*) and historical risk regions in the Czech Republic. Šumar. List 135, 477–486 (2011).
5. Yuan, M. L. et al. Mitochondrial phylogeny, divergence history and high-altitude adaptation of grassland caterpillars (Lepidoptera: Lymantriinae: *Gynaephora*) inhabiting the Tibetan Plateau. Mol. Phylogenet. Evol. 122, 116–124 (2018).
6. Zhang, Q. L. & Yuan, M. L. Research status and prospect of grassland caterpillars (Lepidoptera:Lymantriidae). Pratacult. Sci. 30, 638–646 (2013). (in Chinese)

7. Zhou, Y. & Yin, X. C. Taxonomic study on the steppe caterpillars (Lepidoptera: Lymantriidae). Entomotaxonomia 1, 23–28 (1979). (in Chinese)
8. Yan, L. Studies of taxonomy, geographic distribution in *Gynaephora* genus and life-history strategies on *Gynaephora menyuansis*. Ph.D. Thesis, Lanzhou Universtiy, Lanzhou, China, 2006. (in Chinese)
9. Zhang, Q. L. et al. Gene sequence variations and expression patterns of mitochondrial genes are associated with the adaptive evolution of two *Gynaephora* species (Lepidoptera: Lymantriinae) living in different high-elevation environments. Gene 610, 148–155 (2017).
10. Strathdee, A. T. & Bale, S. Life on the edge:Insect ecology in arctic environments. Annu. Rev. Entomol. 43, 85–106 (1998).
11. Grimaldi, D. & Engel, M. S. *Evolution of the Insects*. Cambridge: Cambridge University Press. 2005.
12. Meier, R. & Lim, G. S. Conflict, convergent evolution, and the relative importance of immature and adult characters in endopterygote phylogenetics. Annu. Rev. Entomol. 54, 85–104 (2009).
13. Xue, S. & Hua, B. Z. Morphology of egg and larva of the semi-looper *Autographa nigrisigna* (Walker) (Lepidoptera: Noctuidae: Plusiinae). Zool. Anz. 277, 162–168 (2018).
14. Vegliante, F. & Hasenfuss, I. Morphology and diversity of exocrine glands in lepidopteran larvae. Annu. Rev. Entomol. 57, 187–204 (2012).
15. Mahlerová, K., Jakubec, P., Novák, M. & Růžička, J. Description of larval morphology and phylogenetic relationships of *Heterotemna tenuicornis* (Silphidae). Sci. Rep-UK. 11, 16973 (2021).
16. Cardoso, L. W., Mielke, C. G. C. & Duarte, M. Morphology of the egg and larva of a poorly known hawkmoth: Subsidies for a better understanding of the systematics of Ambulycini (Lepidoptera: Sphingidae, Smerinthinae). Zool. Anz. 266, 14–22 (2017).
17. Hebert, P. D. N., Cywinska, A., Ball, S. L. & deWaard J. R. Biological identifications through DNA barcodes. P. Roy. Soc. B-Biol. Sci. 270, 313–321 (2003).
18. Leal, W. S. Odorant reception in insects: Roles of receptors, binding proteins, and degrading enzymes. Annu. Rev. Entomol. 58, 373–391 (2013).
19. Field, L., Pickett, J. & Wadhams, L. Molecular studies in insect olfaction. Insect Mol. Biol. 9, 545–551 (2000).
20. Fatouros, N.E., Dicke, M., Mumm, R., Meiners, T. & Hilker, M. Foraging behavior of egg parasitoids exploiting chemical information. Behav. Ecol. 19, 677–689 (2008).
21. Todd, M. G., Paul, Z. G., Alicia, E. T., Roxanne, F., Lisa, L. & Alexander, P. C. Identification of Heliothine (Lepidoptera: Noctuidae) larvae intercepted at U.S. ports of entry from the new world. Econ. Entomol. 112, 603–615 (2019).
22. Wang, Z. H. & Jiang, L. Ultramorphology of the mature larvae of *Sericinus montela* Grey (Lepidoptera: Papilionidae), with descriptions of osmeterium using a novel method of larval preservation. Nat. Hist. 57, 38–53 (2023).
23. Zhao, L., Bao, Z. H. & Lu, L. Ultrastructure of the sensilla on larval antennae and mouthparts in the peach fruit moth, *Carposina sasakii* Matsumura (Lepidoptera: Carposinidae). Micron 42, 478–83

(2011).

24. Gilson, R. P. M., Oleg, G. G., Júlia, F. & Gislene, L. G. A peculiar new species of gall-inducing, clearwing moth (Lepidoptera, Sesiidae) associated with *Cayaponia* in the Atlantic Forest. *Zookeys* 24, 39 – 63 (2019).
25. Liu, L., Zhang, Y., Yan, S. C., Yang, B. & Wang, G. R. Ultrastructural and Descriptive Study on the Adult Body Surface of *Heortia vitessoides* (Lepidoptera: Crambidae). Insects 14, 687 (2023).
26. Barsagade, D. D., Khurad, A. M. & Chamat, M. V. Microscopic structure of mouth parts sensillae in the fifth instar larvae of Erisilkworm, *Philosamia ricini* (Lepidoptera:Saturniidae). *Entomol. Zool.* 1, 15 – 21 (2013).
27. Kristoffersen, L., Hallberg, E., Wallén, R. & Anderbrant, O. Sparse sensillar array on *Trioza apicalis* (Homoptera, Triozidae) antennae—An adaptation to high stimulus levels? Arthropod Struct. Dev. 35, 85–92 (2006).
28. Rougerie, R. & Estradel, Y. Morphology of the preimaginal stages of the african emperor moth *Bunaeopsis licharbas* (Maassen and Weyding): phylogenetically informative characters within Saturniinae (Lepidoptera: Saturniidae). Morphology 269, 207–232 (2008).
29. Matsuoka, Y. J., Murugesan, S. N., Prakash, A. & Monteiro, A. Lepidopteran prolegs are novel traits, not leg homologs. Sci. Adv. 9, 41 (2023).
30. Common, I. F. B. *Moths of Australia*. Melbourne: Melbourne University Press. 1990.
31. Liu, J. X., Zhao, D., Hu, H. R., Liu, Y. Y., Zhao, S. C. & Jiang, L. Biology and morphology of the larvae of *Uropyia meticulodina* (Lepidoptera: Notodontidae), with discussion on their feeding and defensive strategies. Zoomorphology 142, 453–463 (2023).
32. Lin, Y. C., Lin, R. J., Braby, M. F. & Hsu, Y. F. Evolution and losses of spines in slug caterpillars (Lepidoptera: Limacodidae). Ecol. Evol. 9, 9827–9840 (2019).
33. Wagner, D. L. *Caterpillars of Eastern North America: a guide to identifcation and natural history*. Princeton University Press. 2005.
34. Deml, R. & Dettner, K. Extrusible glands and volatile components of the larval gypsy moth and other tussock moths (Lepidoptera.Lymantriidae). Entomol. Gen. 19, 239–252 (1995).
35. Deml, R. Morphological details of the larval “funnel warts” of *Lymantria dispar* (Linnaeus, 1758) (Lepidoptera: Lymantriidae). Entomol. Z. 110, 168–170 (2000).
36. Reinhold, D. & Konrad, D. Comparative morphology and evolution of the funnel warts of larval Lymantriidae (Lepidoptera). Arthropod Struct. Dev. 30, 15–26 (2001).
37. Aldrich, R., Schaefer, W., Oliver, J. E., Puapoomchareon, P., Lee, C. J. & Vander Meer, R. K. Biochemistry of the exocrine secretion fromgypsy moth caterpillars (Lepidoptera: Lymantriidae). Ann. Entomol. Soc. Am. 90, 75–82 (1997).
38. Deml, R. & Dettner, K. Chemical defence of emperor moths andtussock moths (Lepidoptera: Saturniidae, Lymantriidae). Entomol. Gen. 21, 225–251 (1997).

39. Deml, R. & Dettner, K. “Balloon hairs” of gipsy moth larvae (Lepidoptera: Lymantriidae): morphology and comparative chemistry. Comp. Biochem. Phys. B. 112, 673–681 (1995).
40. Yan L., Jiang, X. & Wang, G. Characterization of larvae develop mentin *Gynaephora menyuanensis* (Lepidoptera: Lymantriidae). Acta Pratacult. Sci. 14, 116–120 (2005). (in Chinese)
41. Folmer, O., Black, M., Hoeh, W., Lutz, R. & Vrijenhoek, R. DNA primers for amplification of mitochondrial cytochrome coxidase subunit I from diverse metazoan invertebrates. Mol. Mar. Biol. Biotech. 3, 294–299 (1994).
42. Jeanmougin, F., Thompson, J. D., Gouy, M., Higgins, D. G. & Gibson, T. J. Multiple sequence alignment with Clustal X. Trends Biochem. Sci. 23, 403 (1998).
43. Hall, T. A. BioEdit: a user-friendly biological sequence alignment editor and analysis program for Windows 95/98/NT. Nucleic. Acids. Res. 41, 95–98 (1999).
44. Tamura, K., Peterson, D., Peterson, N., Stecher, G., Nei, M. & Kumar, S. MEGA5: molecular evolutionary genetics analysis using maximum likelihood, evolutionary distance, and maximum parsimony methods. Mol. Biol. Evol. 28, 2731–2739 (2011).
45. Jiang, L. & Hua, B. Z. Morphological comparison of the larvae of *Panorpa obtusa* Cheng and *Neopanorpa lui* Chou & Ran (Mecoptera: Panorpidae). Zool. Anz. 255, 62–70 (2015).
46. Qu, Z. F., Jia, Z. C. & Jiang, L. Description of the third instar larva of the stag beetle *Prismognathus dauricus* Motschulsky, 1860 (Coleoptera: Scarabaeoidea: Lucanidae) using electron microscopy. Micron 120, 10–16 (2019).

Figures

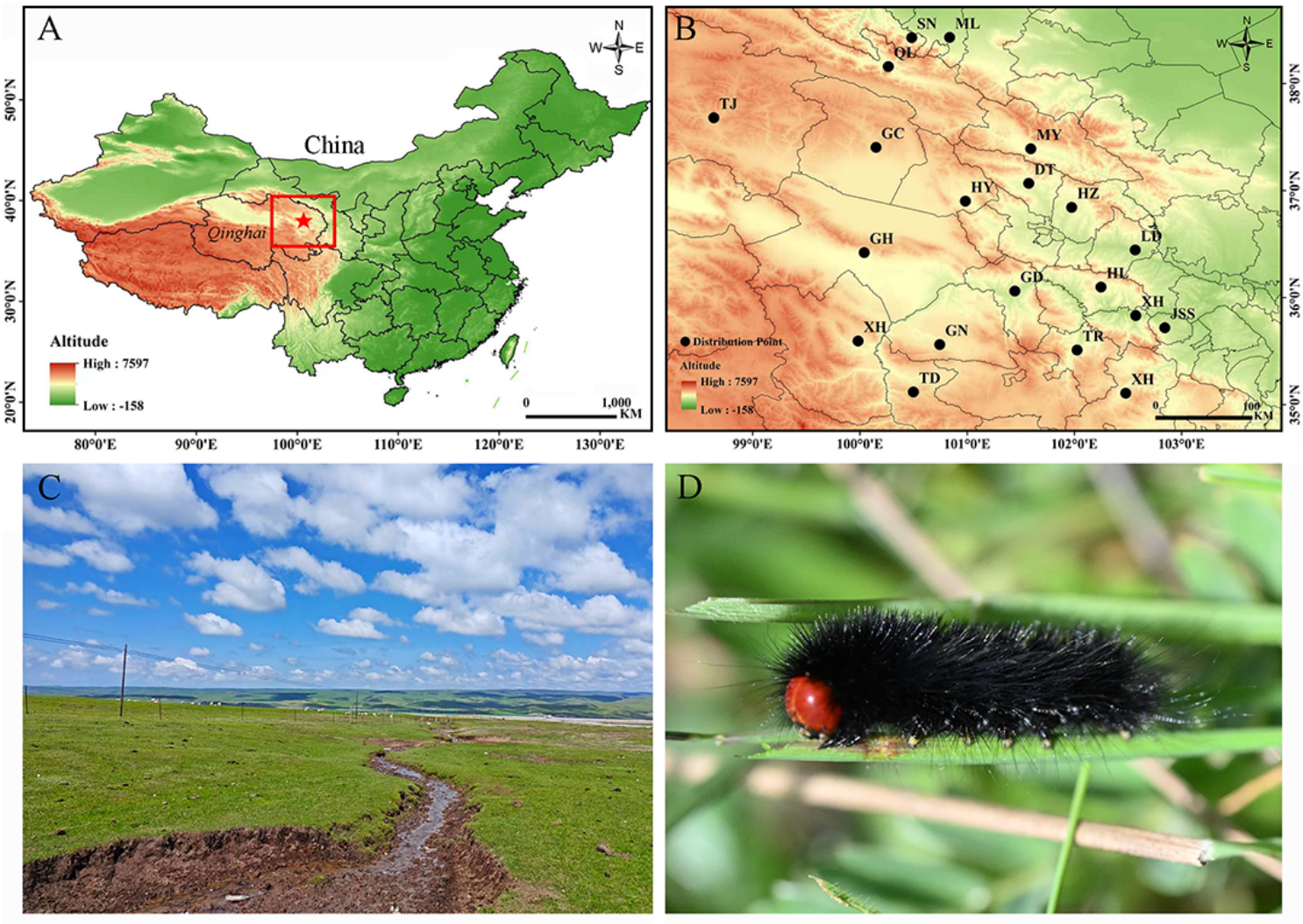

Figure 1

Distribution, habitats, and host plants of *G. menyuanensis*. (A) Distribution in China; (B) collection sites; (C) habitats; (D) feeding on host plants.

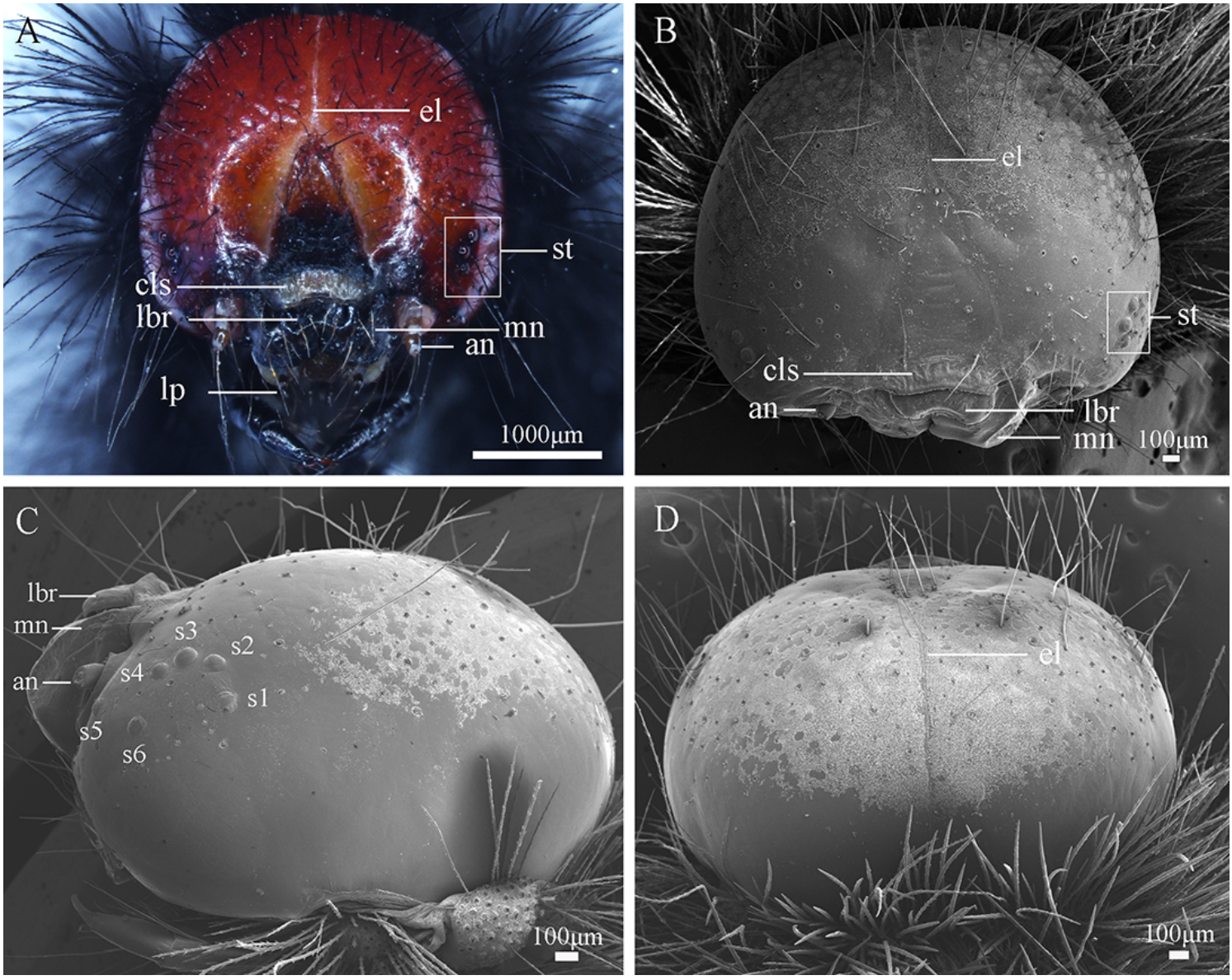

Figure 2

Light micrograph and scanning electronmicroscopy of heads of the last instar larva of *G. menyuanensis*. (A) Frontal view light microscopy; (B) anterior view; (C) lateral view; (D) dorsal view. an: antenna; cls: clypeus; el: ecdysial line; lbr: labrum; lp: labial palp; mn: mandible; st: stemmata; s1–s6: stemma.

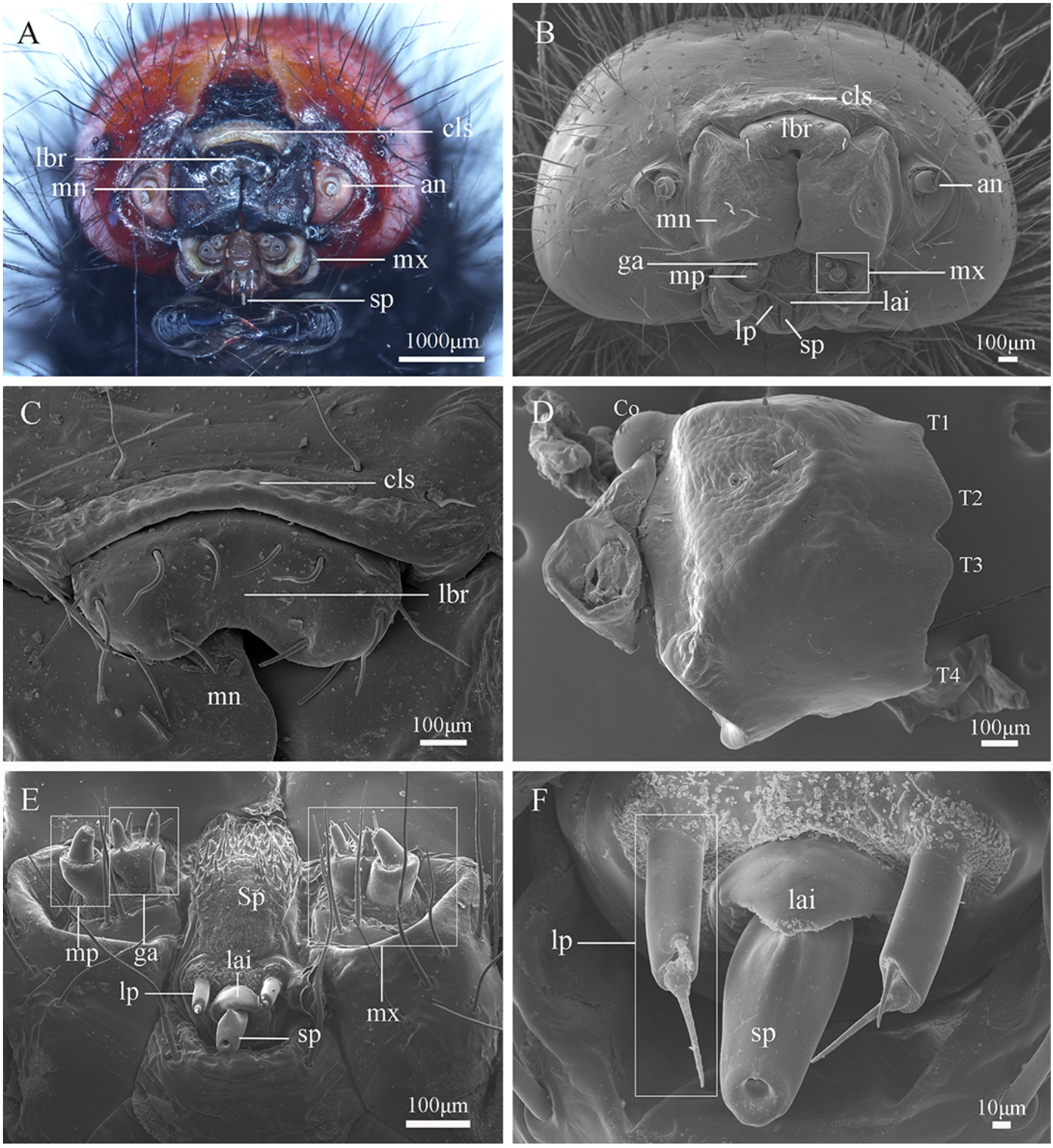

Figure 3

Mouthparts of the last instar larva of *G. menyuanensis*. (A) Light micrograph of frontal view; (B) Scanning electron microscopy of the frontal view: (C) clypeus and labrum; (D) left mandible; (E) maxillary palp and galea; (F) spinneret and labial palp. an: antenna; cls: clypeus; co: condyle; ga: galea; lai: labium; lbr: labrum; lp: labial palp; mn: mandible; mp: maxillary palp; mx: maxilla; sp spinneret; T1–T4: tooth; Sp: spicule.

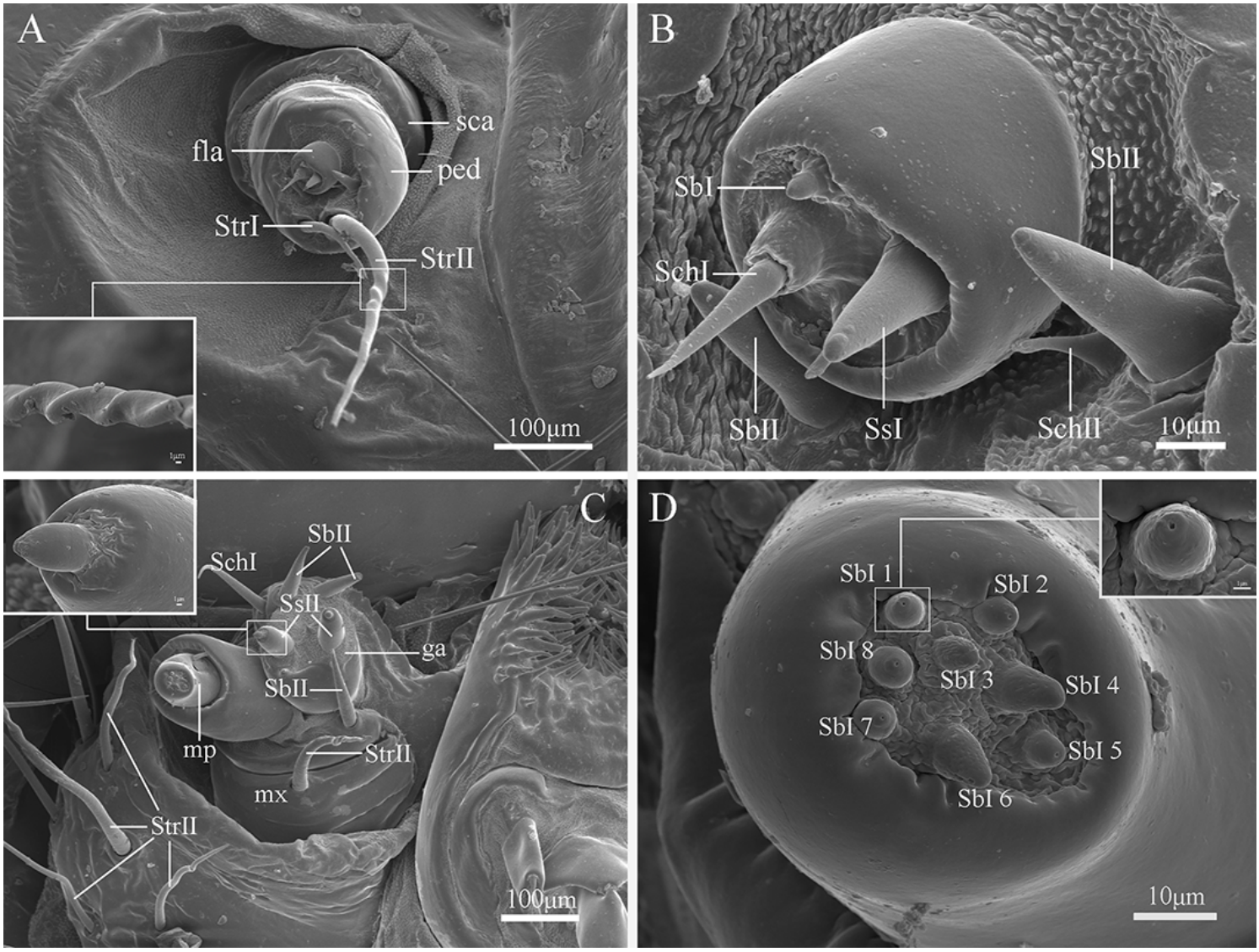

Figure 4

Sensilla in the antenna and mouthparts of the last instar larvae of *G. menyuanensis.* (A) Antenna; (B) sensilla in the flagellum; (C) sensilla in the maxillae; (D) sensilla in the maxillary palp. fla: flagellum; ga: galea; mp: maxillary palp; mx: maxilla; ped: pedicel; sca: scape; Sb: sensilla basiconica; Sch: sensilla chaetica; Ss: sensilla styloconica; Str: sensilla trichodea.

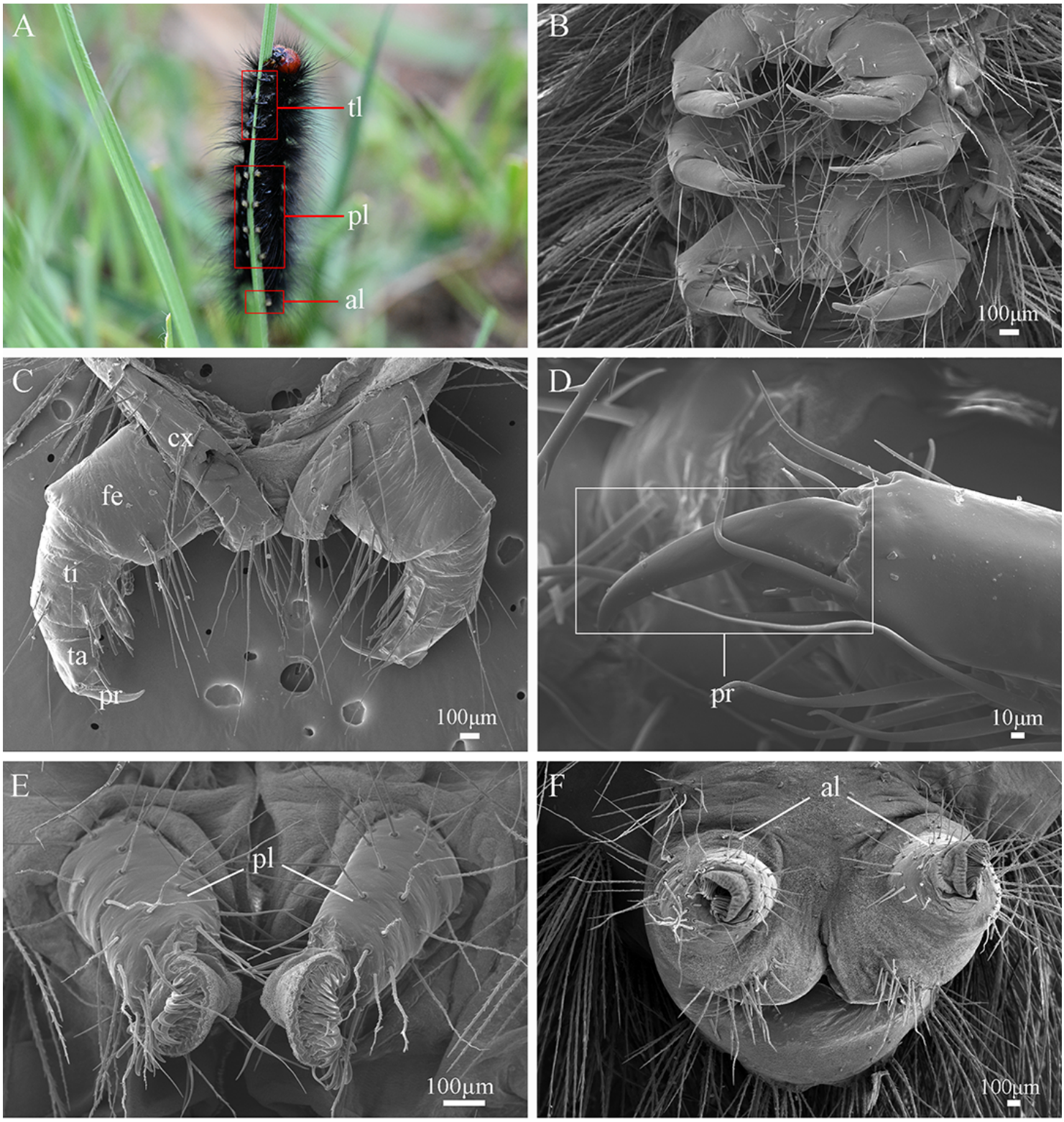

Figure 5

Thoracic legs and prolegs of the last instar larvae of *G. menyuanensis.* (A) Light micrograph of the last instar larva; (B) three pairs of thoracic legs; (C) a pair of thoracic legs; (D) pretarsus magnification; (E) abdominal prolegs; (F) anal prolegs. al: anal prolegs; cx: coxa; fe: femur; pl: prolegs; pr: pretarsus; ta: tarsus; ti: tibia; tl: thoracic legs.

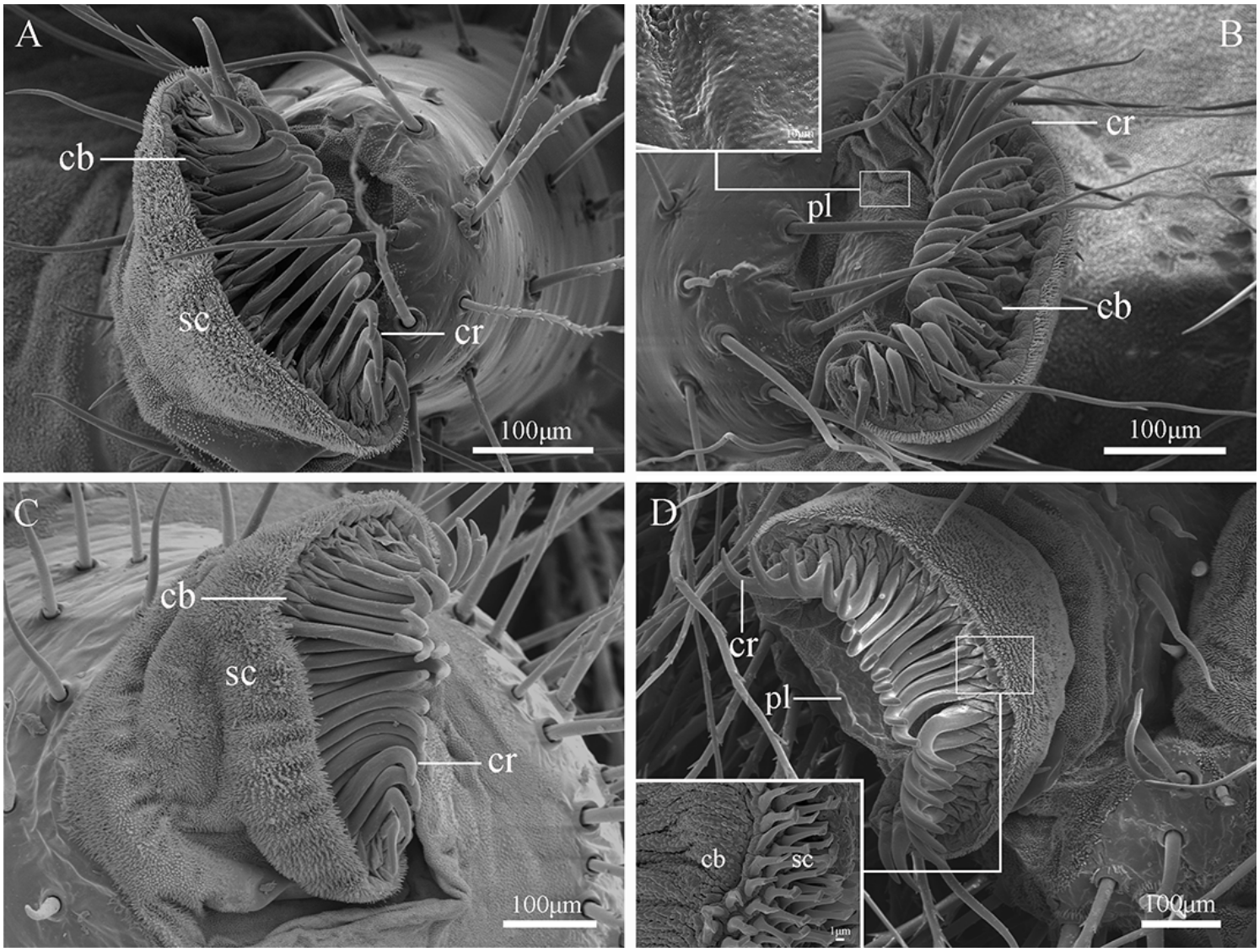

Figure 6

Abdominal and anal prolegs of the last instar larvae of *G. menyuanensis.* (A) Abdominal prolegs magnification; (B) planta; (C) anal prolegs magnification; (D) anal prolegs crochets. al: anal prolegs; cb: coronal blisters; cr: crochets; pl: planta; sc: subcorona.

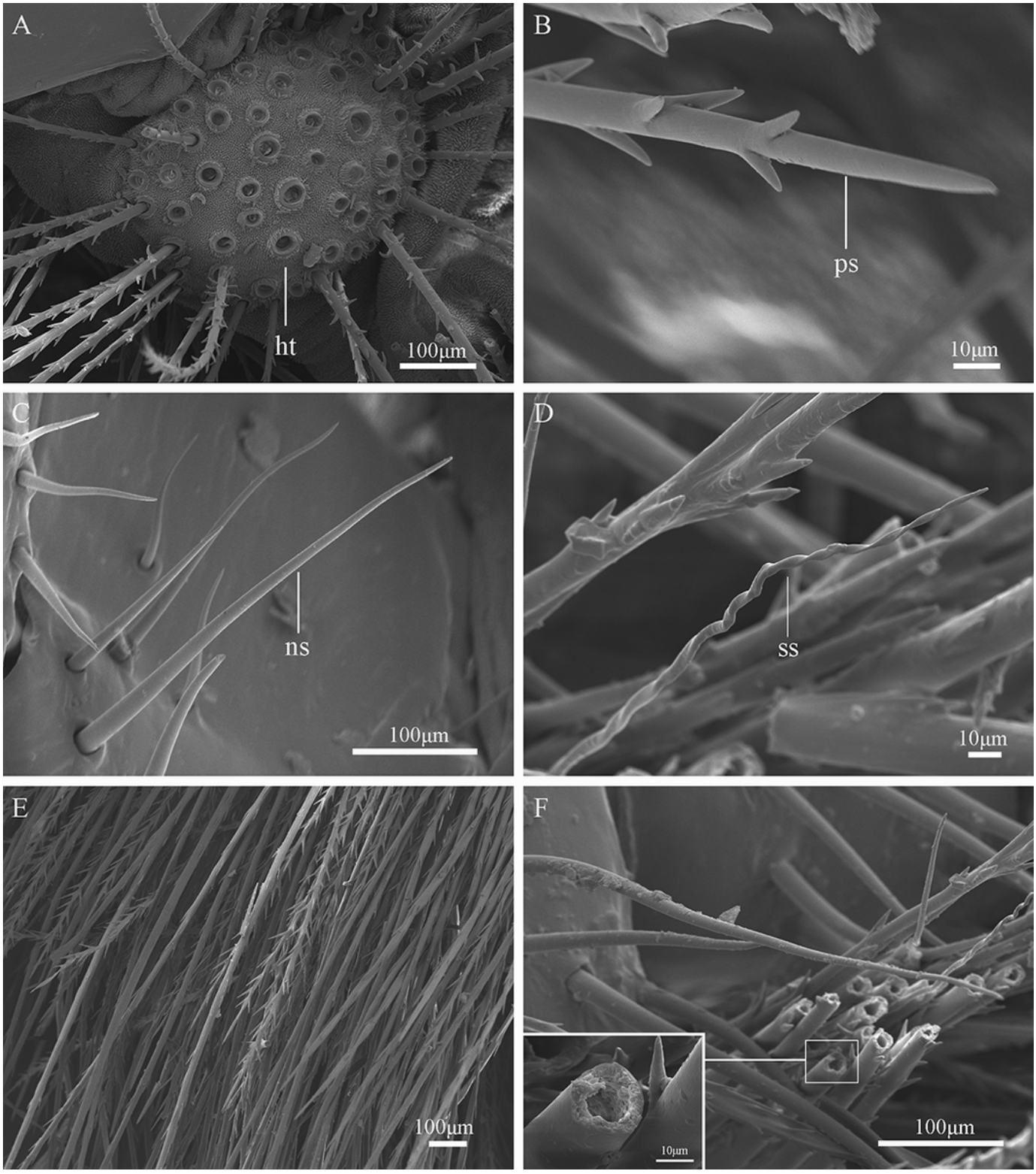

Figure 7

The setae of the last instar larvae of *G. menyuanensis*. (A) Hair tufts; (B) penniform seta; (C) needle-shaped seta; (D) spiral-shaped seta; (E) setae plexus; (F) hollow setae magnification. ht: hair tufts; ns: needle-shaped setae; ps: penniform setae; and ss: spiral-shaped setae.

Figure 8

Funnel warts of the last instar larva of *G. menyuanensis*. (A) Yellow funnel warts; (B) red funnel warts; (C) yellow funnel warts light micrograph; (D) red funnel warts light micrograph; (E) Funnel warts scanning electron microscope; (F) funnel warts magnification. fw: funnel warts; fwa: funnel wall.

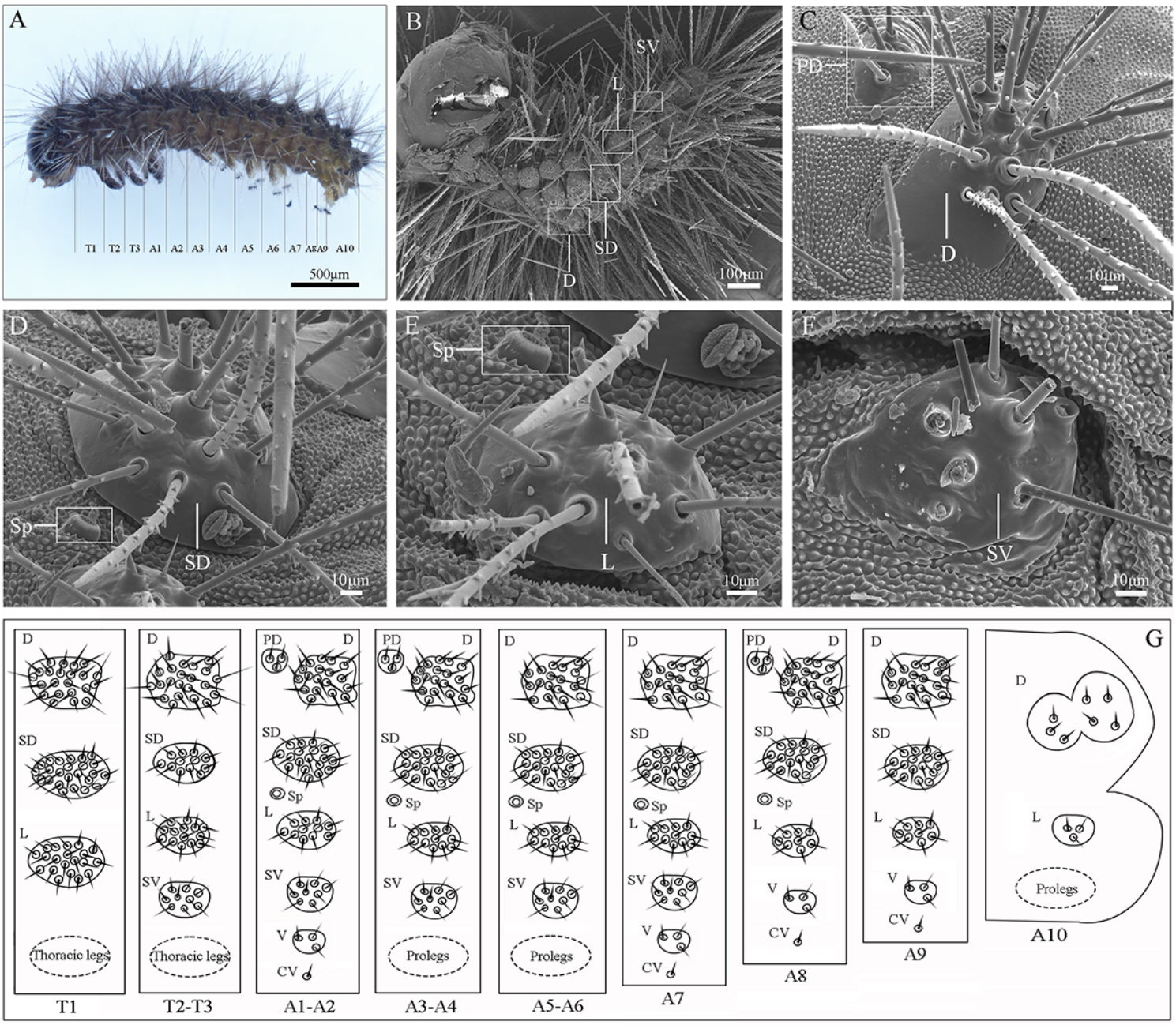

Figure 9

The distribution diagram of the cluster of the first instar larva of *G. menyuanensis*. (A) First instar larva light micrograph; (B) first instar larva scanning electron microscope: (C) dorsal cluster; (D) subdorsal cluster; (E) lateral cluster; (F) subventral cluster; (G) first-instar larva chaetotaxy. D: dorsal cluster; PD: predorsal. cluster; SD: subdorsal cluster; L: lateral cluster; SV: subventral cluster; V: ventral cluster; CV: central ventral cluster; Sp: spiracle; T1: prothorax; T2, T3: meso- and meta-thorax; A1–A10: abdominal segment.

Supplementary Files

This is a list of supplementary files associated with this preprint. Click to download.

- SupplementarymaterialsGrasslandcaterpillaroflarvaeultramorphologySEM2024.1.22.pdf